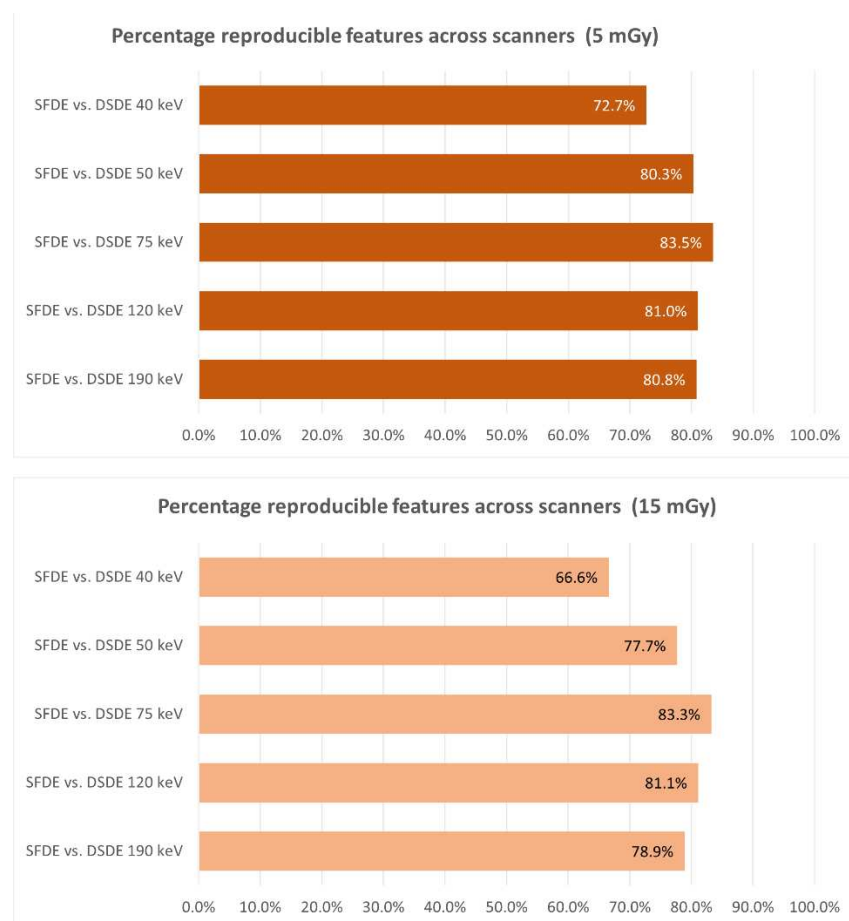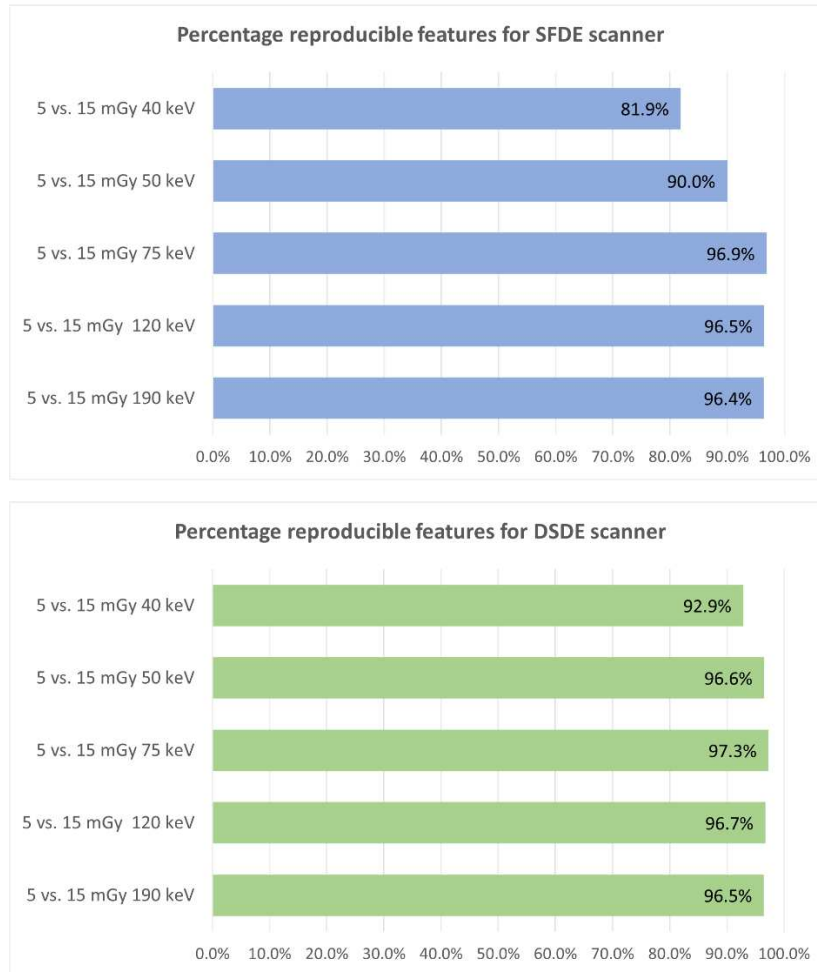*Supplemental Material for the Article:*

Virtual Monoenergetic Images of Dual-Energy CT – Impact on Repeatability, Reproducibility, and Classification in Radiomics

André Euler, MD [1]*, **Fabian Christopher Laqua [2]***, **Davide Cester, PhD [3]**, **Niklas Lohaus, MD [4]**, **Thomas Sartoretti, BSc [5]**, **Daniel Pinto dos Santos, MD [6]**, **Hatem Alkadhi, MD, MPH, EBCR, FESER [7]**, and **Bettina Baessler, MD [8]**

Supplementary Fig. S1: Reproducibility of radiomic features between different dual-energy CT scanners. Bar plots showing the percentage of reproducible features at equal VMI energies between SFDE and DSDE as a function of radiation dose. The highest percentage of reproducible features was achieved at VMI energies of 75 keV and the lowest at 40 keV.

Percentage reproducible features for SFDE scanner

5 vs. 15 mGy 40 keV	81.9%
5 vs. 15 mGy 50 keV	90.0%
5 vs. 15 mGy 75 keV	96.9%
5 vs. 15 mGy 120 keV	96.5%
5 vs. 15 mGy 190 keV	96.4%

Percentage reproducible features for DSDE scanner

5 vs. 15 mGy 40 keV	92.9%
5 vs. 15 mGy 50 keV	96.6%
5 vs. 15 mGy 75 keV	97.3%
5 vs. 15 mGy 120 keV	96.7%
5 vs. 15 mGy 190 keV	96.5%

Supplementary Fig. S2: Reproducibility of radiomic features between different radiation doses
Bar plots showing the percentage of reproducible features at equal VMI energies between 5 and 15mGy for both DECT approaches. Overall, reproducibility was high, except for 40keV of SFDE. Highest reproducibility was achieved at 75 keV.
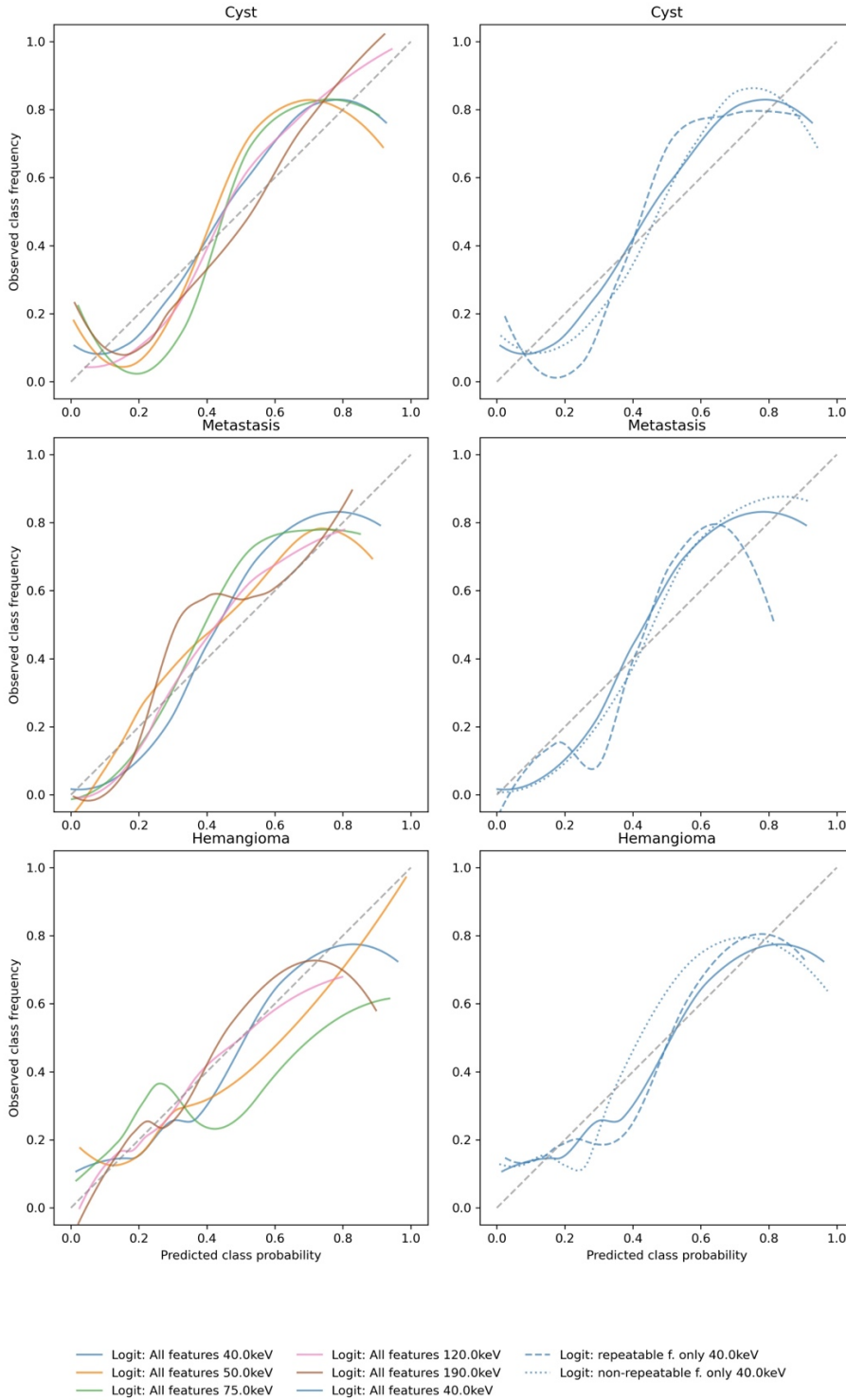
Supplementary Fig. S3: Calibration plot of the penalized logistic regression model for classification of cysts, metastases, and hemangioma by VMI energy (left column) and feature subset (right column), respectively. Color indicates VMI energy. Line style indicates used feature subset ('all features', 'repeatable only' 'non-repeatable only') at 40keV. For every class (hemangioma, cysts, and metastasis) the actual frequency of the occurrence (y-axis) is plotted over the predicted probability. Calibration is considered good when the curve is close to the diagonal. Departure to the top means that for predictions with this value the model underestimates the probability of an occurrence. Analog for departure to the bottom.
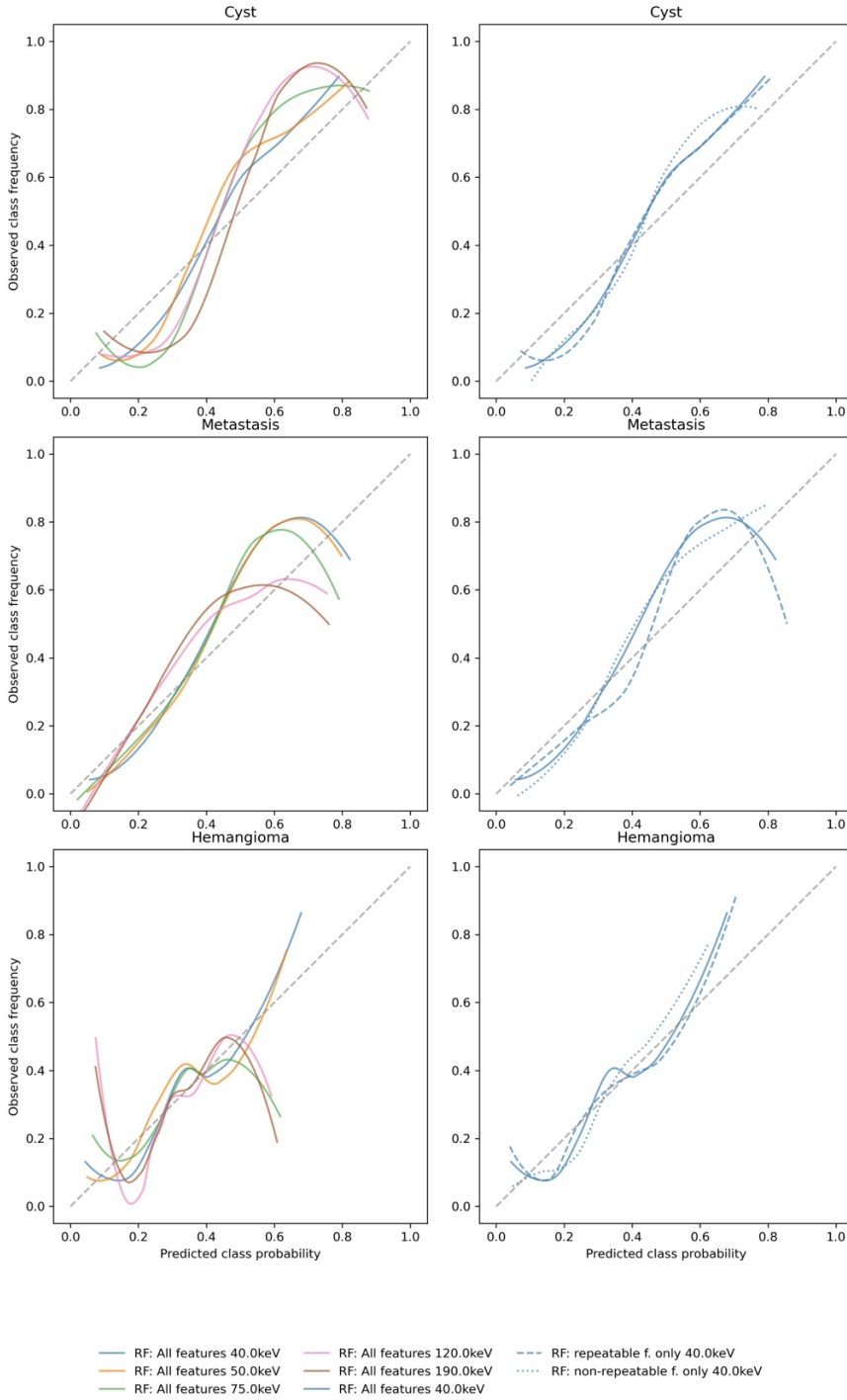
Supplementary Fig. S4: Calibration plot of the random forest model for classification of cysts, metastases, and hemangioma by VMI energy (left column) and feature subset (right column), respectively. Color indicates VMI energy. Line style indicates used feature subset ('all features', 'repeatable only' 'non-repeatable only') at 40keV. For every class (hemangioma, cysts, and metastasis) the actual frequency of the occurrence (y-axis) is plotted over the predicted probability. Calibration is considered good when the curve is close to the diagonal. Departure to the top means that for predictions with this value the model underestimates the probability of an occurrence. Analog for departure to the bottom.
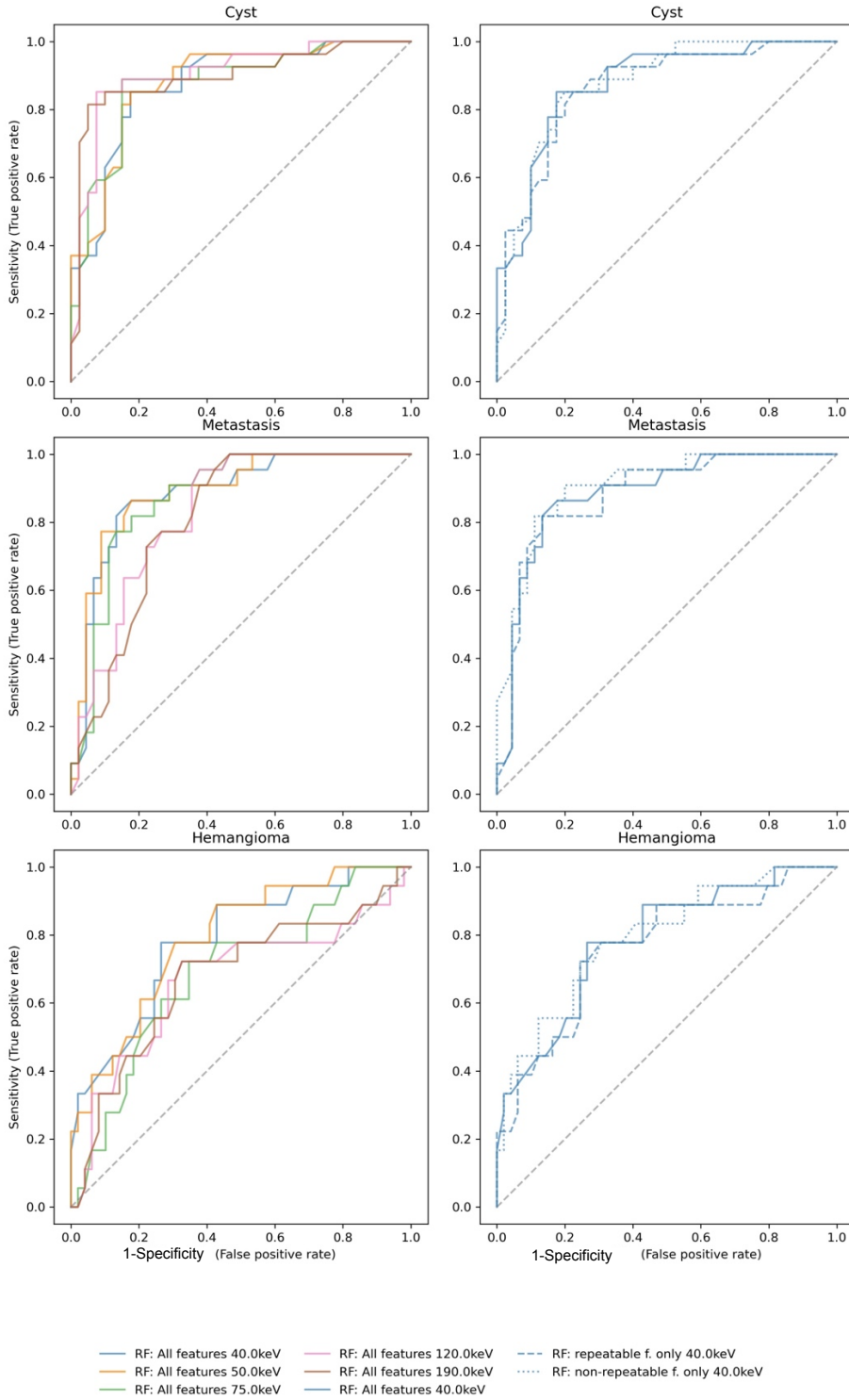
Supplementary Fig. S5: Receiver-operating-characteristics of the random forest model for classification of cysts, metastases, and hemangioma by VMI energy (left column) and feature subset (right column), respectively. Color indicates VMI energy. Line style indicates used feature subset ('all features', 'repeatable only' 'non-repeatable only') at 40keV.

Table S1: Extracted radiomic feature classes with corresponding feature names.

Feature family	Feature name
Intensity-based statistical (histogram) features	Mean (discretized) intensity
	(Discretized) intensity variance
	(Discretized) intensity skewness
	(Excess) (discretized) intensity kurtosis
	Median (discretized) intensity
	Minimum (discretized) intensity
	10th (discretized) intensity percentile
	90th (discretized) intensity percentile
	Maximum (discretized) intensity
	(Discretized) intensity interquartile range
	(Discretized) intensity range
	(Discretized) intensity-based mean absolute deviation
	(Discretized) intensity-based robust mean absolute deviation
	(Discretized) intensity-based median absolute deviation
	(Discretized) intensity-based coefficient of variation
	(Discretized) intensity-based quartile coefficient of dispersion
	(Discretized) intensity-based energy
	Root mean square (discretized) intensity
Intensity-volume histogram features	Volume at intensity fraction
	Intensity at volume fraction
	Volume fraction difference between intensity fractions
	Intensity fraction difference between volume fractions
	Area under the IVH curve
Shape features	VoxelVolume
	Maximum3DDiameter
	MeshVolume
	MajorAxisLength
	Sphericity
	LeastAxisLength
	Elongation
	SurfaceVolumeRatio
	Maximum2DDiameterSlice
	Flatness
	SurfaceArea
	MinorAxisLength
	Maximum2DDiameterColumn
	Maximum2DDiameterRow
Grey level co-occurrence matrix (GLCM)	Joint maximum
	Joint average
	Joint variance
	Joint entropy
	Difference average
	Difference variance
	Difference entropy
	Sum average
	Sum variance
	Sum entropy
	Angular second moment

	Contrast
	Dissimilarity
	Inverse difference
	Normalized inverse difference
	Inverse difference moment
	Normalized inverse difference moment
	Inverse variance
	Correlation
	Autocorrelation
	Cluster tendency
	Cluster shade
	Cluster prominence
	Information correlation 1
	Information correlation 2
Grey level run length matrix (GLRLM)	Short runs emphasis
	Long runs emphasis
	Low grey level run emphasis
	High grey level run emphasis
	Short run low grey level emphasis
	Short run high grey level emphasis
	Long run low grey level emphasis
	Long run high grey level emphasis
	Grey level non-uniformity
	Normalized grey level non-uniformity
	Run length non-uniformity
	Normalized run length non-uniformity
	Run percentage
	Grey level variance
	Run length variance
	Run entropy
Grey level size zone matrix (GLSZM)	Grey level size zone
	Large zone emphasis
	Low grey level zone emphasis
	High grey level zone emphasis
	Small zone low grey level emphasis
	Small zone high grey level emphasis
	Large zone low grey level emphasis
	Large zone high grey level emphasis
	Grey level non-uniformity
	Normalized grey level non-uniformity
	Zone size non-uniformity
	Normalized zone size non-uniformity
	Zone percentage
	Grey level variance
	Zone size variance
	Zone size entropy
Grey level distance zone matrix (GLDZM)	Small distance emphasis
	Large distance emphasis
	Low grey level zone emphasis
	High grey level zone emphasis
	Small distance low grey level emphasis
	Small distance high grey level emphasis
	Large distance low grey level emphasis

	Large distance high grey level emphasis
	Grey level non-uniformity
	Normalized grey level non-uniformity
	Zone distance non-uniformity
	Normalized zone distance non-uniformity
	Zone percentage
	Grey level variance
	Zone distance variance
	Zone distance entropy
Neighborhood grey tone difference matrix (NGTDM)	Coarseness
	Contrast
	Busyness
	Complexity
	Strength
Neighboring grey level dependence matrix (NGLDM)	Low dependence emphasis
	High dependence emphasis
	Low grey level count emphasis
	High grey level count emphasis
	Low dependence low grey level emphasis
	Low dependence high grey level emphasis
	High dependence low grey level emphasis
	High dependence high grey level emphasis
	Grey level non-uniformity
	Normalized grey level non-uniformity
	Dependence count non-uniformity
	Normalized dependence count non-uniformity
	Dependence count percentage
	Grey level variance
	Dependence count variance
	Dependence count entropy
	Dependence count energy

Each feature was extracted as an original feature as well as using wavelet transform in 8 decompositions and Laplacian of Gaussian filters with sigma values from 1 to 5. For mathematical definitions of all features, please refer to the recommendations of the Image Biomarker Standardization Initiative (IBSI) (Zwanenburg et al., 2020, 2016)

Table S2: In-vitro classification performance metrics for penalized logistic regression by feature subset, DECT scanner, radiation dose, and VMI energy.

Features	Scanner	Dose [mGy]	Energy [keV]	AUC	Brier score (BS)	R² (scaled BS)
all	DSDE	5	40	1.0 (1.0;1.0)	0.00024 (6e-07;0.00092)	1.0 (1.0;1.0)
			50	1.0 (1.0;1.0)	0.0002 (5.3e-07;0.00073)	1.0 (1.0;1.0)
			75	1.0 (1.0;1.0)	0.00019 (5.4e-07;0.00068)	1.0 (1.0;1.0)
			120	1.0 (1.0;1.0)	0.00013 (5.8e-07;0.00045)	1.0 (1.0;1.0)
			190	1.0 (1.0;1.0)	0.00013 (4.6e-07;0.00045)	1.0 (1.0;1.0)
		15	40	1.0 (1.0;1.0)	0.0001 (3.6e-07;0.00034)	1.0 (1.0;1.0)
			50	1.0 (1.0;1.0)	0.00011 (3.4e-07;0.00036)	1.0 (1.0;1.0)
			75	1.0 (1.0;1.0)	0.00012 (5.8e-07;0.00042)	1.0 (1.0;1.0)
			120	1.0 (1.0;1.0)	0.00013 (5.2e-07;0.00044)	1.0 (1.0;1.0)
			190	1.0 (1.0;1.0)	0.00012 (8.5e-07;0.0004)	1.0 (1.0;1.0)
	SFDE	5	40	1.0 (1.0;1.0)	0.00024 (6.3e-07;0.00087)	1.0 (1.0;1.0)
			50	1.0 (1.0;1.0)	0.00022 (5.1e-07;0.00084)	1.0 (1.0;1.0)
			75	1.0 (1.0;1.0)	0.00019 (4.6e-07;0.00071)	1.0 (1.0;1.0)
			120	1.0 (1.0;1.0)	0.00021 (3.9e-07;0.00077)	1.0 (1.0;1.0)
			190	1.0 (1.0;1.0)	0.00019 (3.7e-07;0.00066)	1.0 (1.0;1.0)
		15	40	1.0 (1.0;1.0)	0.00014 (6.9e-07;0.0005)	1.0 (1.0;1.0)
			50	1.0 (1.0;1.0)	0.00012 (7.1e-07;0.00043)	1.0 (1.0;1.0)
			75	1.0 (1.0;1.0)	0.00016 (5.1e-07;0.00055)	1.0 (1.0;1.0)
			120	1.0 (1.0;1.0)	0.00015 (3.4e-07;0.00054)	1.0 (1.0;1.0)
			190	1.0 (1.0;1.0)	0.00017 (4.9e-07;0.0006)	1.0 (1.0;1.0)
repeatable	DSDE	5	40	1.0 (1.0;1.0)	0.00012 (1.4e-07;0.00045)	1.0 (1.0;1.0)
			50	1.0 (1.0;1.0)	0.00014 (1.6e-07;0.00054)	1.0 (1.0;1.0)
			75	1.0 (1.0;1.0)	9.7e-05 (1.4e-07;0.00036)	1.0 (1.0;1.0)
			120	1.0 (1.0;1.0)	8.1e-05 (1.7e-07;0.0003)	1.0 (1.0;1.0)
			190	1.0 (1.0;1.0)	8.5e-05 (1.7e-07;0.00032)	1.0 (1.0;1.0)
		15	40	1.0 (1.0;1.0)	0.00015 (3.2e-07;0.00055)	1.0 (1.0;1.0)
			50	1.0 (1.0;1.0)	0.00014 (2.7e-07;0.00051)	1.0 (1.0;1.0)
			75	1.0 (1.0;1.0)	0.00013 (3.4e-07;0.00048)	1.0 (1.0;1.0)

			120	1.0 (1.0;1.0)	0.00015 (4e-07;0.00054)	1.0 (1.0;1.0)
			190	1.0 (1.0;1.0)	0.00012 (4.3e-07;0.00046)	1.0 (1.0;1.0)
	SFDE	5	40	1.0 (1.0;1.0)	0.00022 (1.3e-07;0.00082)	1.0 (1.0;1.0)
			50	1.0 (1.0;1.0)	0.00019 (1.5e-07;0.00075)	1.0 (1.0;1.0)
			75	1.0 (1.0;1.0)	0.00012 (1.5e-07;0.00046)	1.0 (1.0;1.0)
			120	1.0 (1.0;1.0)	0.00011 (1.7e-07;0.00043)	1.0 (1.0;1.0)
			190	1.0 (1.0;1.0)	0.00011 (1.4e-07;0.00042)	1.0 (1.0;1.0)
		15	40	1.0 (1.0;1.0)	0.00018 (1.5e-07;0.00061)	1.0 (1.0;1.0)
			50	1.0 (1.0;1.0)	0.00011 (1.2e-07;0.0004)	1.0 (1.0;1.0)
			75	1.0 (1.0;1.0)	0.00012 (1.3e-07;0.00045)	1.0 (1.0;1.0)
			120	1.0 (1.0;1.0)	0.00013 (1.5e-07;0.00048)	1.0 (1.0;1.0)
			190	1.0 (1.0;1.0)	0.00014 (1.5e-07;0.00052)	1.0 (1.0;1.0)
non-repeatable	DSDE	5	40	0.99 (1.0;0.9)	0.11 (0.011;0.31)	0.83 (0.5;0.98)
			50	1.0 (1.0;0.97)	0.066 (0.004;0.17)	0.89 (0.71;0.99)
			75	1.0 (1.0;1.0)	0.04 (0.0025;0.11)	0.93 (0.81;1.0)
			120	1.0 (1.0;1.0)	0.022 (0.0013;0.051)	0.96 (0.91;1.0)
			190	1.0 (1.0;1.0)	0.034 (0.0015;0.11)	0.94 (0.81;1.0)
		15	40	1.0 (1.0;0.96)	0.092 (0.00069;0.28)	0.85 (0.48;1.0)
			50	1.0 (1.0;0.99)	0.054 (0.0015;0.12)	0.91 (0.79;1.0)
			75	1.0 (1.0;0.96)	0.15 (0.00085;0.4)	0.76 (0.31;1.0)
			120	0.99 (1.0;0.94)	0.14 (0.003;0.42)	0.78 (0.33;0.99)
			190	0.98 (1.0;0.88)	0.25 (0.0051;0.64)	0.61 (-0.0022;0.99)
	SFDE	5	40	1.0 (1.0;1.0)	0.011 (0.00022;0.028)	0.98 (0.91;1.0)
			50	0.99 (1.0;0.9)	0.15 (0.015;0.44)	0.77 (0.25;0.98)
			75	0.98 (1.0;0.86)	0.19 (0.0043;0.56)	0.7 (0.0;0.99)
			120	0.99 (1.0;0.89)	0.17 (0.013;0.59)	0.73 (0.092;0.98)
			190	1.0 (1.0;0.96)	0.11 (0.0021;0.48)	0.82 (0.25;1.0)
		15	40	1.0 (1.0;1.0)	0.044 (0.00027;0.34)	0.93 (0.49;1.0)
			50	0.98 (1.0;0.8)	0.18 (0.011;0.69)	0.72 (0.01;0.98)
			75	0.96 (1.0;0.74)	0.31 (0.031;0.67)	0.52 (-0.11;0.94)

120	0.98 (1.0;0.86)	0.2 (0.013;0.52)	0.69 (0.074;0.98)
190	0.98 (1.0;0.86)	0.17 (0.02;0.49)	0.73 (0.13;0.97)